

RESEARCH PAPER

 OPEN ACCESS 

Autologous decellularized extracellular matrix promotes adipogenic differentiation of adipose derived stem cells in low serum culture system by regulating the ERK1/2-PPAR γ pathway

Yao Qian^{ib}, Hao Chen^b, Tianyun Pan^c, Tian Li^b, Zikai Zhang^b, Xuling Lv^b, Jingping Wang^b, Ziwan Ji^b, Yucang He^b, Liqun Li^b, and Ming Lin^a

^aDepartment of Plastic Surgery, The First Affiliated Hospital of Wenzhou Medical University, Wenzhou City, China; ^bDepartment of Pathology, Huzhou Hospital of Traditional Chinese Medicine, Huzhou City, China; ^cDepartment of Obstetrics and Gynecology, The Second Affiliated Hospital and Yuying Children's Hospital of Wenzhou Medical University, Wenzhou City, China

ABSTRACT

High viability and further adipogenic differentiation of adipose-derived stem cells (ADSCs) are fundamental for engraftment and growth of the transplanted adipose tissue. It has been demonstrated that extracellular matrix (ECM) regulates cell proliferation and differentiation by interacting with ERK1/2 signalling pathway. In this study, we prepared autologous decellularized extracellular matrix (d-ECM) and explored its effect on the proliferation and adipogenic ability of ADSCs in low serum culture. We found that 2% foetal bovine serum (FBS) in growth medium inhibited cell viability and DNA replication, and decreased mRNA and protein levels of PPAR γ and C/EPB α compared with 10% FBS. Correspondingly, after 14-days adipogenic induction, cells cultured in 2% FBS possessed lower efficiency of adipogenesis and expressed less adipocyte differentiation markers ADIPOQ and aP2. On the contrary, the d-ECM-coated substrate continuously promoted the expression of PPAR γ , and regulated the phosphorylation of ERK1/2 in different manners during differentiation. Pretreatment with ERK1/2 inhibitor PD98059 neutralized the effects of d-ECM, which suggested d-ECM might regulate the adipogenesis of ADSCs through ERK1/2-PPAR γ pathway. In addition, d-ECM was revealed to regulate the transcription and expression of stemness-associated genes, such as OCT4, NANOG and SOX2, in the undifferentiated ADSCs, which might be related to the initiation of differentiation.

ARTICLE HISTORY

Received 23 July 2020
Revised 14 March 2021
Accepted 17 March 2021

KEYWORDS

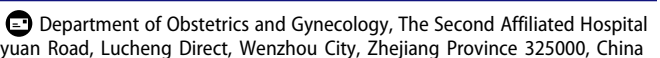
Adipose-derived stem cells; extracellular matrix; cell proliferation; adipogenic differentiation; ERK1/2-PPAR γ pathway

Introduction

Adipose derived stem cells (ADSCs) have been widely applied in the field of regenerative medicine because of their easy accessibility and potentials of self-renewal and multidirectional differentiation [1]. It is well known that early transplanted ADSCs will suffer from nutrition deficiency, which negatively influences the survival of stem cells and leads to an unsatisfied effect of cell-assisted lipotransfer [2]. Foetal bovine serum (FBS), full of bioactive proteins and growth factors as well as hormones, is a common medium composition for cell culture. It was demonstrated in the previous study that higher concentration of FBS was accompanied by an increase in PPAR γ expression [3]. Epigenetic evidence suggests that, compared with mesenchymal stem cells (MSCs) cultured in autologous serum (AS), cells in FBS exhibit a hypomethylation of histone H3 at lysine 9 (H3K9) in the promoter of Ppar γ gene and a hyperacetylation of H3K9 in that of

adiponectin gene [4]. Therefore, FBS may contribute to a suitable microenvironment for adipogenic gene transcription and subsequent adipogenesis. It is of great significance for clinical applications to promote the proliferation and adipogenesis of ADSCs facing serum restriction.

Extracellular matrix (ECM) is a complex architecture surrounding cells and consists of different proportions of structural proteins, adhesive proteins, and glycans. ECM from diverse sources regulates cell proliferation, migration and differentiation in different manners. Zhang et al. found that ECM secreted from ADSCs cultured in growth medium contained more fibronectin (FN) while that from cells in adipogenic medium was rich in laminin (LM). These two kinds of ECM, respectively, promoted cell migration or adipogenic differentiation of the reseeded cells [5]. Lee et al. found that ECM deposited by Mile Sven 1 endothelial cells (MS1) delayed cell proliferation but accelerated the process of

CONTACT Ming Lin  LMLML600@163.com; Liqun Li  wz.llq@163.com 

© 2021 The Author(s). Published by Informa UK Limited, trading as Taylor & Francis Group.

This is an Open Access article distributed under the terms of the Creative Commons Attribution-NonCommercial License (<http://creativecommons.org/licenses/by-nc/4.0/>), which permits unrestricted non-commercial use, distribution, and reproduction in any medium, provided the original work is properly cited.

differentiation in comparison with MSCS-derived ECM [6].

There is accumulating evidence indicating that ECM components can activate the multiple differentiation potential of stem cells. Bone marrow derived mesenchymal cells (BMSCs) that were seeded onto the autologous cell-free extracellular matrix expressed more stem cell surface markers and could differentiate into multilineage cells better once cultured in the differentiation medium [7]. It was reported that autologous ECM permitted the chondrogenic differentiation of BSMCs even without any exogenous growth factors [8]. Compared to the conventional plastic culture materials, the substrates coated with ECM may possess stiffness that is more appropriate for differentiation [9]. In addition, it was reported that the reseeded cells on d-ECM expressed more integrin subunits including α 5-7 on their surface, which may influence the intracellular signalling pathways mediating differentiation [5].

Extracellular signal-regulated kinase 1/2 (ERK1/2), as a member of the mitogen activated protein kinases (MAPK), plays a significant role in regulating cell proliferation, migration and differentiation. With variations of the duration and extent of MAPK activation, different stimuli will drive cell fate towards two different developments: proliferation or differentiation [10]. As a downstream target of ERK1/2, PPAR γ can in turn phosphorylate ERK1/2 by binding to the EGFR receptor, which enhances the mRNA transcription of PPAR γ [11]. The interaction between ERK1/2 and PPAR γ may facilitate or hinder adipogenic differentiation under different experimental conditions [12,13]. Given the fact that PPAR γ regulates the transcript levels of many adipogenic genes such as adiponectin [14], it is very possible that this protein attends to the ERK1/2-associated adipogenesis.

Activation of ERK1/2 and generation of ECM reinforce each other. Mechanical stress and stretch can prompt cells to secrete more matrix components including collagen (COL) I–IV and FN as well as aggrecan by ERK1/2 pathway [15,16]. Recently, it has been demonstrated in a series of studies that ERK1/2 signalling pathway stimulates the production of matrix of cell species including smooth muscle cell and mesangial cell as well as nucleus pulposus cell, thus involved in the pathogenesis of many diseases such as pulmonary hypertension [17], diabetic nephropathy [18] and intervertebral disc degeneration [19]. ECM components, in turn, can influence cellular behaviour by regulating ERK1/2 pathway. A study based on a suspension culture system showed that adding ECM powder increased the ERK1/2 activity and improved the survival of mesenchymal progenitor cells in the

early formed spheroids [20]. It was also reported that ECM fabricated by small intestinal submucosa promoted cell proliferation and osteoblastic differentiation of rat BMSCs through Smad1/5/8 and ERK1/2 signalling pathways [21]. Moreover, our previous study reported that autologous decellularized extracellular matrix (d-ECM) not only increased the viability but enhanced adipogenic differentiation of ADSCs exposed to H₂O₂ [22]. However, whether ERK1/2 pathway is involved in the adipogenic process of ADSCs reseeded on d-ECM still remains unclear.

In this study, cell viability, proliferation and morphology were examined to reveal the effects of d-ECM on ADSCs in low serum culture. Apart from Oil Red O staining, the adipocyte-specific transcription factors PPAR γ and C/EPB α keeping active during adipogenesis, and adiponectin (ADIPOQ) and adipocyte fatty acid binding protein (aP2) that express robustly in the mature adipocytes were selected as indicators to evaluate the adipogenic ability of ADSCs, as described in a previous study [23]. Since stem cell status may intervene in the relation between the potential to proliferate and differentiate [24], the expression of pluripotent markers including OCT4, NANOG and SOX2 was examined simultaneously.

Materials and methods

Cell isolation and culture

Adipose tissue was obtained from the liposuction operations performed in the First Affiliated Hospital of Wenzhou Medical University in the period from November 2020 to December. The patients were randomly selected and included five adult females aged from 23 to 45. All patients signed the informed consent for scientific research and publication. Isolation of ADSCs was performed as described in our previous work [25]. Briefly, adipose tissue was fully cut with a scissor and digested using 0.1% collagenase type I (SCR103, Sigma, USA) at 37°C for 40 min. Then, the mixture was sequentially filtered using a 100 and a 200 mesh strainers. The filtrate was collected and centrifuged at room temperature at 250 g for 5 min. Finally, the pellet was resuspended in complete medium (HUXMD-90,011, Cyagen Biosciences, USA) and transferred into a plastic cell culture flask. The cells were cultured at 37°C with 5% CO₂, and observed under a CKX41 inverted phase-contrast microscope (Olympus, JPN). The medium was changed every 3 days, and cells were passaged when reaching 90% confluence. The 3rd passage ADSCs were used for cell

identification and d-ECM preparation, and the 5th passage ones were used for the subsequent experiments.

Multi-lineage differentiation induction

In the adipogenesis or osteogenesis assay, cells were, respectively, cultured in Human Mesenchymal Stem Adipogenic Differentiation Medium (supplemented with insulin, dexamethasone, 3-isobutyl-1-methyl-xanthine and indometacin) (GUXMX-90,031, Cyagen Biosciences, USA) or Osteogenic Differentiation Medium (supplemented with dexamethasone, b-glycerophosphate and L-ascorbic acid-2-phosphate) (GUXMX-90,021, ditto for supplier) for 2 weeks. Then the cells were fixed with 4% paraformaldehyde and stained with Oil Red O or Alizarin Red according to the manufacturers' instructions.

For the chondrogenesis assay, cells were transferred into a 15-ml centrifuge tube and were centrifuged for 4 min at 250 g at room temperature. Then, the intact cell pellet was carefully transferred into Human Mesenchymal Stem Chondrogenic Differentiation Medium (supplemented with dexamethasone, ascorbate, insulin-transferrin-selenium supplement, sodium pyruvate, proline, TGF- β 3) (GUXMX-90,041, Cyagen Biosciences, USA). After 3 weeks, the firm cell spheroid formed was fixed and sectioned, followed by Alcian Blue staining. The samples were imaged under an OLYMPUS IX71 phase contrast microscope (Olympus Corporation, JPN).

Flow cytometry

The primary antibodies against human cluster of differentiation (CD) markers including CD34 (ab195013, Abcam, UK), CD44 (103,011, BioLegend, USA), CD45 (555,485, BD Biosciences USA) and CD90 (555,595, BD Biosciences, USA), and FITC-conjugated goat anti-rabbit secondary antibody were used in flow cytometry to analyse the profiles of cell surface immunophenotype. Briefly, ADSCs reaching 80–90% confluence were digested with 0.25% Trypsin and washed in PBS twice. Then, the cells were resuspended at a concentration of 1×10^5 /ml and incubated in PBS containing 2% bovine serum albumin (B2064, Sigma, USA) and 0.1% sodium azide (S2002, Sigma, USA) for 30 min at 4°C. A total of 100 μ L of cell suspension for each sample was incubated in primary antibodies (1:10 dilution) in the dark for 30 min at 4°C, followed by the incubation with secondary antibody (1:100 dilution) under the same condition. Then, the cells were washed in PBS twice and analysed using a FACSVerser flow cytometer (BD Biosciences, USA).

Preparation of decellularized extracellular matrix (d-ECM)

The extracellular matrix deposited by ADSCs was obtained according to the scheme we established before [22]. Briefly, ADSCs were collected and seeded at a density of 1×10^5 or 5×10^4 /well in 12- or 24-well plates (Corning, USA) in complete medium. When the confluence was over 60%, 50 μ M L-ascorbic acid (HY-B0166, MedchemExpress, USA) was added to stimulate matrix production [7]. The medium was changed every 3–4 days, and was discarded one week later. After washed with PBS twice, the samples were decellularized by incubating them in PBS containing 0.5% Triton X-100 (P1080, Solarbio, CHN) and 20 mM NH₄OH (G1822, Solarbio, CHN) for 5 min at 37°C. Afterwards, the samples were washed gently with sterile enzyme-free water (R1600, Solarbio, CHN) three times and were treated with 100 U/ml DNase I (D8071, Solarbio, CHN) for 1 h at 37°C. Following a final three washes, the d-ECM samples were observed under a phase contrast microscope and then stored sterile at 4°C for later use.

Immunofluorescence

The samples treated with or without decellularization were washed with PBS twice and fixed with 4% formaldehyde for 15 min. The samples were blocked with 2% BSA (B2064, Sigma, USA) in PBS for 30 min at room temperature, and were then incubated with anti-fibronectin (250,073, ZENBIO, CHN) and anti-laminin (384,832, ZENBIO, CHN) primary antibodies diluted 1:200 in PBS overnight at 4°C. Sequentially, the samples were incubated with goat anti-mouse/rabbit secondary antibody (BYE010/BYE019, Boyun, CHN) for 1 h at room temperature. After washed with PBS three times, the samples were counterstained with 4,6-diamidino-2-phenylindole (DAPI) (C0065, Solarbio, CHN) and imaged under a DM2500 fluorescent microscope (Leica, GER).

Cell Counting Kit-8 (CCK-8) assay and cell counting assay

For the CCK-8 assay, ADSCs were inoculated at 5×10^4 /well in 24-well plates coated with or without d-ECM in 500 μ L medium containing 0% or 2% foetal bovine serum (FBS, GUXMX-90,031, Cyagen Biosciences, USA), and then cultured for different time (1, 2, 3, 4 days). The cells growing on the plastic substrates in 10% FBS were used as control group. After the indicated culture time, cells in each well were washed with

PBS twice and then incubated in 500 μ L serum-free medium containing 10% CCK-8 reagent (CK04, Dojindo Molecular Technologies, JPN) for 4 h at 37°C. Sequentially, the plates were sufficiently shaken, and a total of 400 μ L mixture for each sample was equally transferred into 4 wells of a 96-well plate. Absorbance values at 450 nm were measured using a SPECTRA max 384 microplate reader (Molecular Devices Corporation, USA) and were then normalized by control group.

For cell counting, cells were seeded at 5×10^4 /well on the plastic or d-ECM substrates of 24-well plates and then cultured in 2% or 10% FBS for 3 days. Afterwards, cells were collected and counted using a Countess II Automated Cell Counter (Thermo Fisher Scientific, USA).

EdU (5-ethynyl-2'-deoxyuridine) staining

ADSCs were treated as described above. Cell-Light Edu Apollp567 In Vitro Kit (C10310, RiboBio, China) was used in this experiment. Briefly, cells in each well of a 24-well plate were washed with PBS three times and incubated in 200 μ L serum-free medium containing 50 μ M EdU for 2 h at 37°C. Then, the cells were washed three times to remove the residual EdU. After that, cells were fixed with 4% paraformaldehyde for 30 min at room temperature and then stained with 200 μ L 1x Apollp567 dye in the dark for 30 min at room temperature. Sequentially, cells were treated with 0.5% TritonX-100 diluted in 100 μ L PBS and were then counterstained using 200 μ L 1x Hoechst33342 for 30 min. Afterwards, the samples were washed with PBS three times and observed under an ECLIPSE TI fluorescent inverted microscope (Nikon, JPN). The result was expressed as the percentage of EdU-positive cells.

Assessment of ADSCs morphology

The long/short axis ratio of cells was calculated to quantitatively evaluate the change of the morphology of ADSCs treated with low-serum culture or d-ECM. For each group, 10 representative cells with unmasked contour were selected at 12 h or 72 h of culture, respectively. According to a previous study [6], the ratios of long axis to short axis of the cells of each sample were calculated using ImageJ 1.8.0 software (National Institutes of Health, USA). The extreme values including the greatest and the smallest values were removed.

Real-Time Polymerase Chain Reaction (RT-PCR)

Gene expression was quantitatively analysed by qRT-PCR. Briefly, the total RNA was extracted from the ADSCs reseeded onto plastic or d-ECM using Trizol Reagent (15,596,018, invitrogen, USA) following the manufacturer's instructions. RNase-Free DNase I (D8071, Solarbio, CHN) was used to remove residual DNA in the sample. Then, reverse transcription was performed using a RevertAid First Strand complementary DNA (cDNA) Synthesis Kit (1622, Thermo, USA). Real-time PCR consisting of initial denaturation (94°C, 10 min) and subsequent 40 cycles (denaturation, 94°C, 20 s; annealing, 55°C, 20 s; extension, 72°C, 20 s) was carried out with 20-fold diluted cDNA sample and 2x SybrGreen qPCR Master Mix (F-415XL, Thermo, USA) in an ABI-7500 Real-Time System (Applied Biosystems, USA). The relative expression levels of target genes were calculated by $2^{-\Delta\Delta CT}$ method with GAPDH as calibrator gene and were normalized to control group (10% FBS). The primer sequences used in the PCR are listed in Table 1.

Western blotting analysis

The protein samples used for this experiment were prepared in two different ways. For matrix component analysis, samples with or without decellularization were lysed in RIPA buffer (Solarbio, CHN) containing 1% phenylmethylsulfonyl fluoride (P0100, Solarbio, CHN) and 1% phosphatase inhibitor (P1260, Solarbio, CHN). In order to remove the cellular debris, the lysate was centrifuged at 14,000 g for 11 min and then boiled in 4x loading buffer (P1015, Solarbio, CHN) for 5 min. For protein analysis, cells were seeded at 1×10^5 /well on the plastic or d-ECM substrates of 12-well plates in medium containing 2% FBS, and then cultured for 3 days. In order to inhibit ERK1/2 signaling pathway, 50 μ M PD98059 (HY-12,028, Medchemexpress, USA) dissolved in 0.1% dimethyl sulphoxide (DMSO) was added at least 2 h prior to

Table 1. Primer sequence of human genes used in this study.

Gene	Primer sequence	Product size (bp)
NANOG	F: 5'-CAGAGAAGAGTGTGCGCAAAAAGGA-3' R: 5'-TGAGGTTCCAGGATGTTGGAGAGTTC-3'	165
SOX2	F: 5'-CGCAGATGCAGCCCATGACCCGCTAC-3' R: 5'-GGCCTCGGACTTGACCACCGAACCCA-3'	170
OCT4	F: 5'-GCCAGAAGGGCAAGCGATCAAGCA-3' R: 5'-GGAAAGGGACCGAGGAGTACAGTG-3'	174
PPAR γ	F: 5'-GACCAAGTAACTCTCTCAAATA-3' R: 5'-TGGGCTCCATAAAGTACCAAAA-3'	163
C/EPB α	F: 5'-CGGTGGACAAGAACAGCAACAGAGT-3' R: 5'-CCTTGACCAAGGAGCTCTGGCA-3'	227
GAPDH	F: 5'-AGAAGGCTGGGCTCATTG-3' R: 5'-AGGGCCATCCACAGTCTTC-3'	258

F: forward direction; R: reverse direction.

the inoculation. Other groups were treated with the same amount of DMSO. The cells cultured in complete medium (10% FBS) were used as control group. Then, cells were harvested for protein extraction. A BCA kit (P0012, Beyotime, CHN) was used to quantify the protein concentration of samples among all groups. Sequentially, protein samples were separated by sodium salt-polyacrylamide gel electrophoresis, followed by Western blotting analysis according to a previous study [5]. Protein bands were visualized using an enhanced chemiluminescence substrate (PE0010, Solarbio, CHN) in a ChemiDoc MP imager (Bio-Rad, USA), and then analysed by Image Lab V3.0 software (Bio-Rad, USA). Equal loading of proteins was demonstrated by GAPDH, and all the band density values were normalized by control group.

The primary antibodies used in this experiment were anti-fibronectin (1:1000, 250,073, ZENBIO), anti-laminin (1:1000, 384,832, ZENBIO), anti-collagen I/III/IV (1:1000, 380,760/R23957/252,404, ZENBIO), anti-OCT4 (1:1000, K005554P, Solarbio), anti-SOX2 (1:1000, K008063P, Solarbio), anti-NANOG (1:1000, K003637P, Solarbio), anti-p-ERK1/2 (1:1000, AF1015, Affinity), anti-ERK1/2 (1:1000, AF0155, Affinity), anti-p-PPAR γ (1:1000, AF3284, Affinity), anti-PPAR γ (1:1000, AF6284, Affinity), anti-C/EPB α (1:1000, AF6333, Affinity), anti-ADIPOQ (1:1000, DF7000, Affinity), anti-aP2 (1:1000, AF0535, Affinity), and anti-GAPDH (1:2000, 380,626, ZENBIO). The secondary antibody used was HRP-conjugated goat anti-rabbit/mouse IgG (1:2000, SE134/SE131, ZENBIO).

Oil Red O staining

After 3-days treatment and 14-days adipogenic induction, cells were fixed with 4% paraformaldehyde and stained with 0.5% Oil Red O solution in the dark for 1 h. The samples were rinsed with 60% isopropanol and photographed under a phase contrast microscope. For each group, three samples were stained and examined. Relative stained area (Area%) and the ratio of integrated density to stained area (IntDen/Area) were calculated for analysis. Afterwards, the samples were destained in 100% isopropanol for 15 min. The supernatant was collected and optical density at 540 nm (OD_{540nm}) was measured using a DU-800 spectrophotometer (BECKMAN, USA).

Statistical analysis

Each experiment in this study was repeated three times. All data, expressed as the means \pm SD, were compared by one-way ANOVA with Tukey's post hoc test using

SPSS Statistics 20.0 software (IBM, USA). P-values <0.05 were considered as statistically significant.

Results

Identification of ADSCs

Morphological phenotype, cluster of differentiation markers and multilineage differentiation potential were determined to identify ADSCs. The 3rd passage cells cultured in complete medium for 3 days appeared spindle-shape and arranged in swirls (Figure 1(a)), which was regarded as a morphological signature of mesenchymal stem cells [26]. After stained with Oil Red O, Alizarin Red and Alcian Blue, the cells cultured in differentiation medium for 2 or 3 weeks were positive for lipid droplets, calcified nodules and acid mucopolysaccharides, which suggested the success of adipogenesis, osteogenesis and chondrogenesis, respectively (Figure 1(a)). Consistent with our previous study [27], the result of flow cytometry showed that the isolated cells were positive for CD44 (99.6%) and CD90 (97.7%) while negative for CD34 (1.6%) and CD45 (1.7%) (Figure 1(b)), which demonstrated these pluripotent cells were non-haematopoietic mesenchymal cells.

Characterization of d-ECM

In our previous work, observation of d-ECM using a scanning electron microscope revealed a fibrous structure that was made up of many cords with the same direction [22]. In this study, we also noticed a similar structure under an inverted microscopes (Figure 2(a)). Immunofluorescence results showed that the fluorescence intensity of LM and DAPI decreased significantly after decellularization, while that of FN did not change obviously. Furthermore, FN was mainly located in the intercellular matrix while LM was distributed more closely to cells (Figure 2(b)), which suggested that LM might be lost during the process of decellularization. The results of Western blotting analysis showed that compared with non-decellularized matrix, d-ECM retained almost all FN and COL I, and partial COL III, COL IV and LM. It seemed that intracellular substance was fully eliminated as GAPDH was not present in the d-ECM samples prepared (Figure 2(c)).

Cell viability and proliferation of ADSCs in growth medium

As showed in the CCK-8 assay, compared with control group (10% FBS), low serum concentrations (0% and

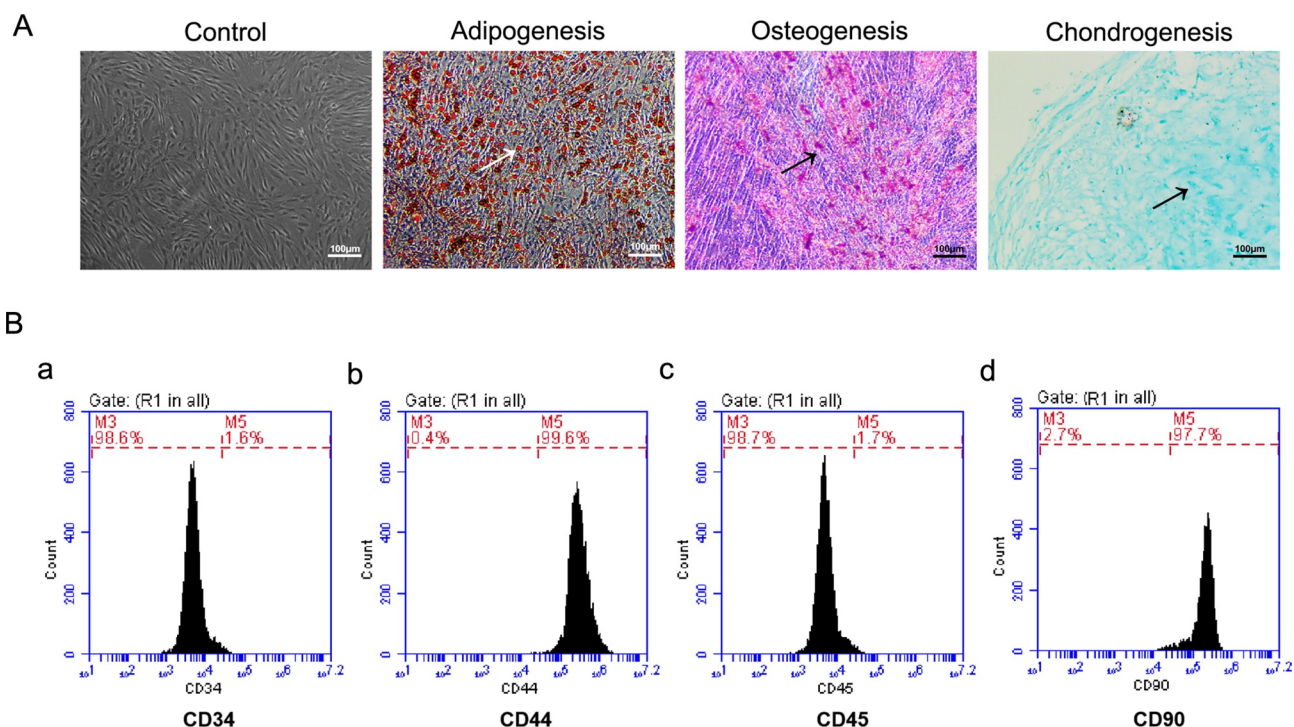


Figure 1. Identification of ADSCs. A. Adipogenesis, osteogenesis and chondrogenesis of the 3th passage ADSCs. The panel on the left presented the morphology and arrangement of the uninduced ADSCs, and the other three ones showed the lipid droplets, calcified nodules and acid mucopolysaccharides in differentiated cells, respectively (marked by the arrows). Bars = 100 μ m. B. ADSCs were immunophenotyped for CD34 (a), CD44 (b), CD45 (c) and CD90 (d) by flow cytometry.

2% FBS) progressively decreased cell viability as the duration of starvation increased, and the trend became stable since day 3 post inoculation. Compared to the plastic material, d-ECM significantly increased cell viability of ADSCs cultured in 2% FBS for 3 days (from $57.9 \pm 2.27\%$ to $72.9 \pm 3.78\%$), but did not influence those in 0% FBS whose viability was decreased severely (Figure 3(a)). Consistent with the result of CCK-8 assay, cell number counting showed that the d-ECM-coated substrates provided more cells ($68.6 \pm 5.17\%$) than the plastic ones ($52.2 \pm 3.54\%$) on day 3 post treatments (Figure 3(b)). Based on the data given above, we used 2% FBS and 3-days culture as the conditions for low serum treatment in the subsequent experiments. In addition, the percentage of EdU-positive cells in 2% FBS plus d-ECM group was increased while no obvious DNA replication occurred in 2% FBS-only group (Figure 3(c)), indicating an accompanying change in cell proliferation.

Morphological change of ADSCs before and after differentiation

Before the adipogenic induction, we found that the ratios of long/short axis of ADSCs increased on the whole with culture time increased. The long/short axis ratios of 2%

FBS group were more concentrated and had no significant difference with 10% FBS group. Compared to the other two groups, ADSCs reseeded on d-ECM possessed larger morphological polarity at both 12 h and 24 h (Figure 3(d)). Although it was difficult to quantify cell morphology after adipogenesis, many 'normal' cells with spindle-shape could be observed in 10% FBS group and d-ECM group. However, ADSCs in 2% FBS group were more slender than the other groups, which was exactly opposite to the situation before differentiation. In addition, the cell density was significantly decreased, and the spindle shape was absent in PD98059 pretreatment group (Figure 6(a)).

Expression of stemness-associated genes of undifferentiated ADSCs

RT-PCR detection revealed that the transcription of NANOG, OCT4 and SOX2 genes was decreased in 10% FBS group in a time-dependent way, but was increased in 2% FBS group. Compared to 2% FBS group, a similar but weaker uptrend was observed in d-ECM treatment group (Figure 4(a)). Western blotting analysis before differentiation confirmed that the protein expression levels of NANOG, OCT4 and SOX2 were increased in 2% FBS group and fallen back by d-ECM treatment (Figure 4(b)), which was consistent with the result of RT-PCR.

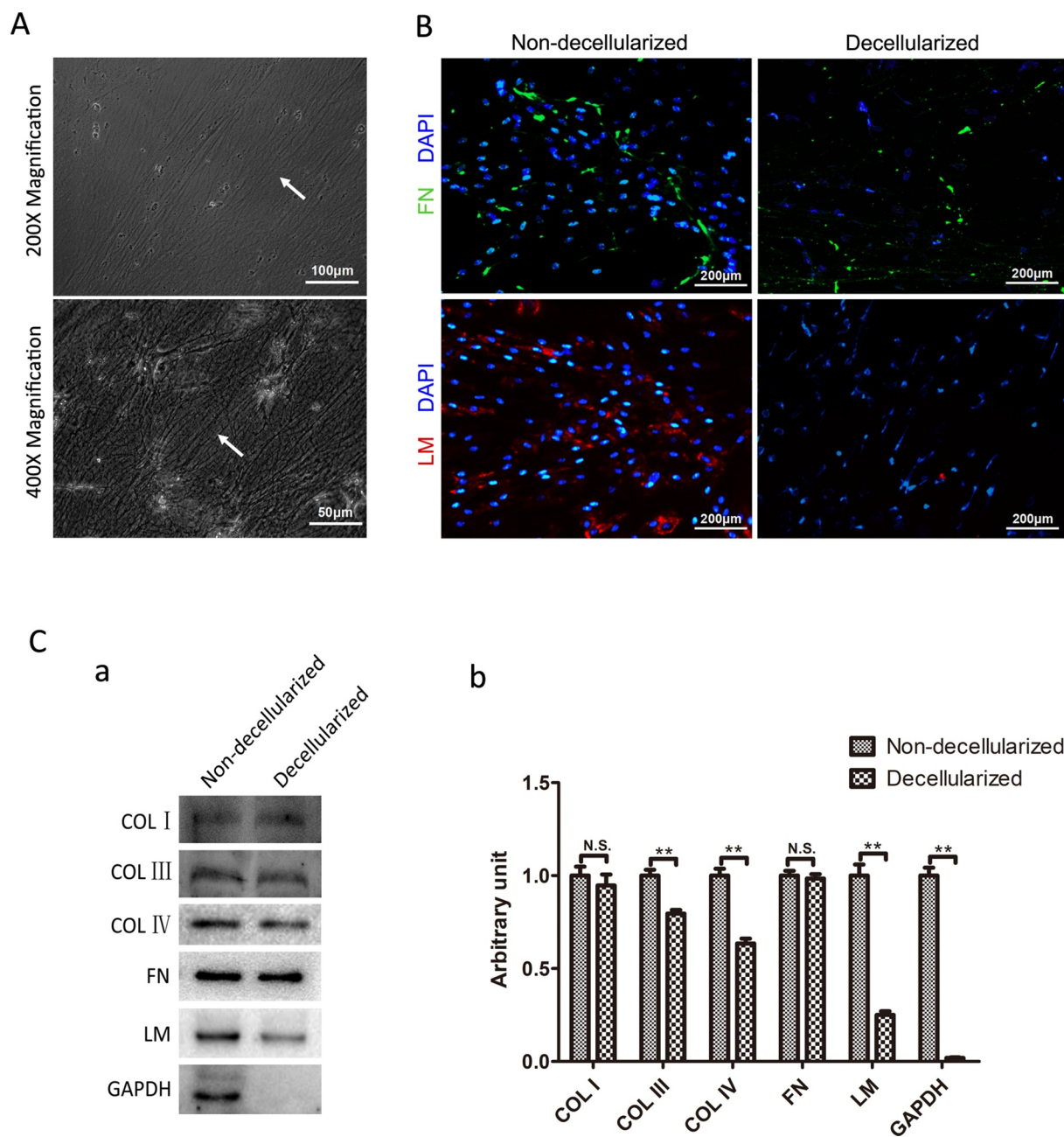


Figure 2. Identification of d-ECM. A. Observation of d-ECM at 200x or 400x magnification. The fibrous structure of d-ECM was marked by the arrows. Bars = 50 or 100 μm . B. FN (green) and LM (red) in d-ECM or non-decellularized ECM were detected using immunofluorescence. Nuclei were stained with DAPI (blue). Bars = 200 μm . C. Component analysis of d-ECM by Western blotting. ECM without decellularization served as the control. **, $p < 0.01$, non-decellularized ECM vs. Decellularized ECM. N.S., not significant as $p > 0.05$. FN, fibronectin; LM, laminin; COL I, collagen I; COL III, collagen III; COL IV, collagen IV.

Phosphorylation of ERK1/2 and expression of adipogenesis-associated genes and proteins before and after differentiation

Before adipogenic induction, as shown in (Figure 4), PPAR γ and C/EPB α mRNA levels among groups did not differ significantly until day 2. Low serum culture (2% FBS) down-regulated the expression levels of mRNA over time, and d-ECM significantly relieved

this decrease (Figure 5(a)). The results of Western blotting confirmed the effects of low FBS concentration on the expression of PPAR γ and C/EPB α , and d-ECM treatment alleviated the 2%-FBS-inducing inhibition of PPAR γ expression. As a selective inhibitor of ERK1/2, PD98059 inhibited the phosphorylation of ERK1/2, accompanied by a decrease in PPAR γ expression. However, it seemed that C/EPB α protein expression

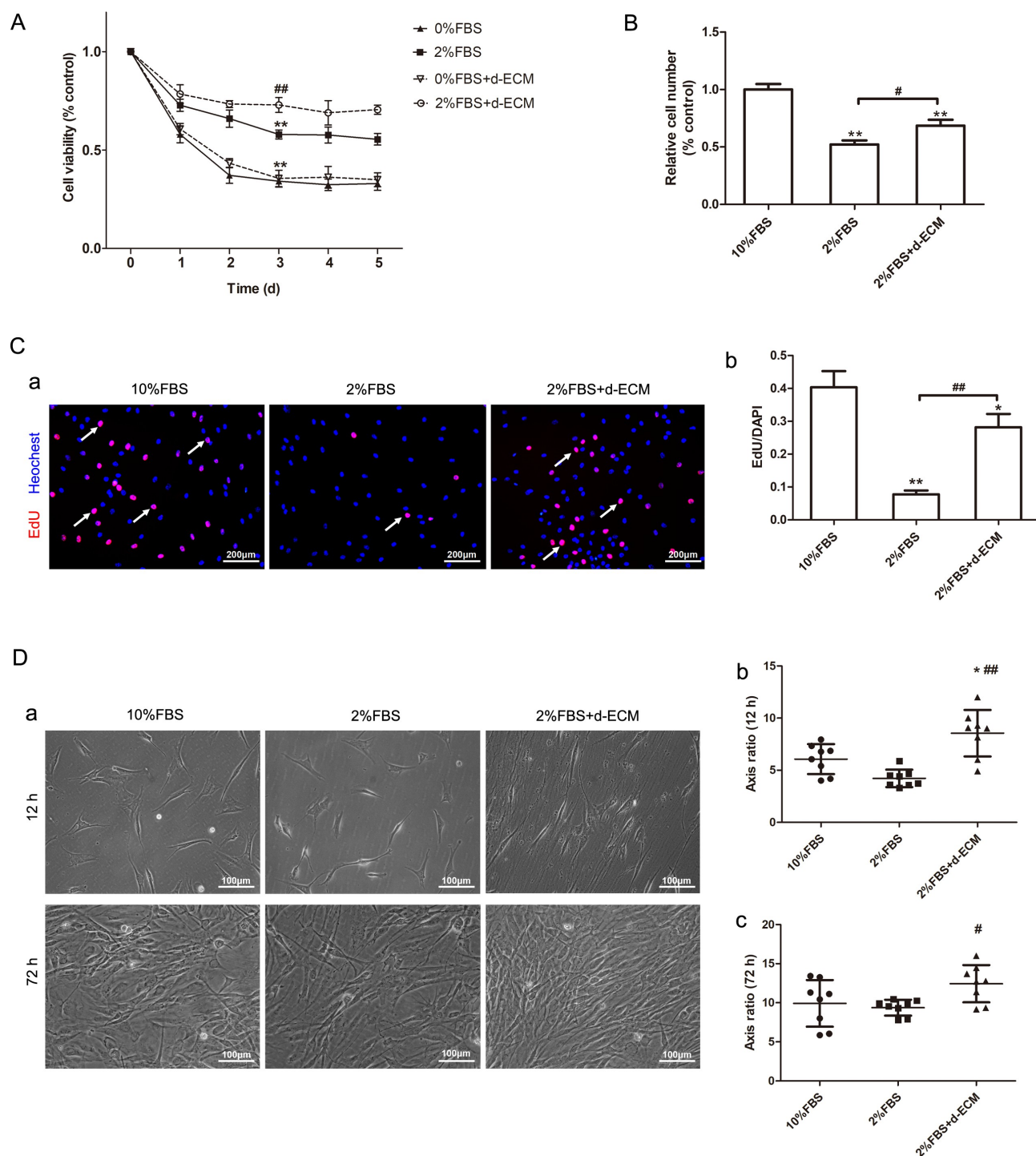


Figure 3. Effects of serum-restriction and d-ECM on cell viability, proliferation and morphology of ADSCs. **A.** ADSCs at the 5th passage were cultured in medium containing 0% or 2% FBS on the plastic or d-ECM-coated surface for 1–5 days, followed by a CCK-8 assay. Cells cultured in complete medium (10% FBS) on the plastic surface were used as control group. $N = 4$. **, $p < 0.01$, 0% or 2% FBS group vs. 10% FBS group; ##, $p < 0.01$, vs. 2% FBS group. **B.** Numbers of ADSCs treated with 2% FBS or d-ECM for 3 days were counted using an automated cell counter. $N = 3$. **, $p < 0.01$, vs. 10% FBS group; #, $p < 0.05$, vs. 2% FBS group. **C.** Cells were grouped according to the ‘cell counting’ experiment, followed by EdU staining and Heochest33342 counterstaining. Red-stained nuclei appeared in the EdU-positive cells (marked by the arrows), which represented a high level of DNA replication. $N = 3$. *, $p < 0.05$, vs. 10% FBS group; **, $p < 0.01$, vs. 10% FBS group; ##, $p < 0.01$, vs. 2% FBS group. Bars = 200 μm . **D.** Cells were treated as above, and observed under an invert microscope at 12 h and 72 h post treatments. Bars = 100 μm . *, $p < 0.05$, vs. 10% FBS group; #, $p < 0.05$, vs. 2% FBS group; ##, $p < 0.01$, vs. 2% FBS group. FBS, foetal bovine serum. EdU, 5-ethynyl-2'-deoxyuridine.

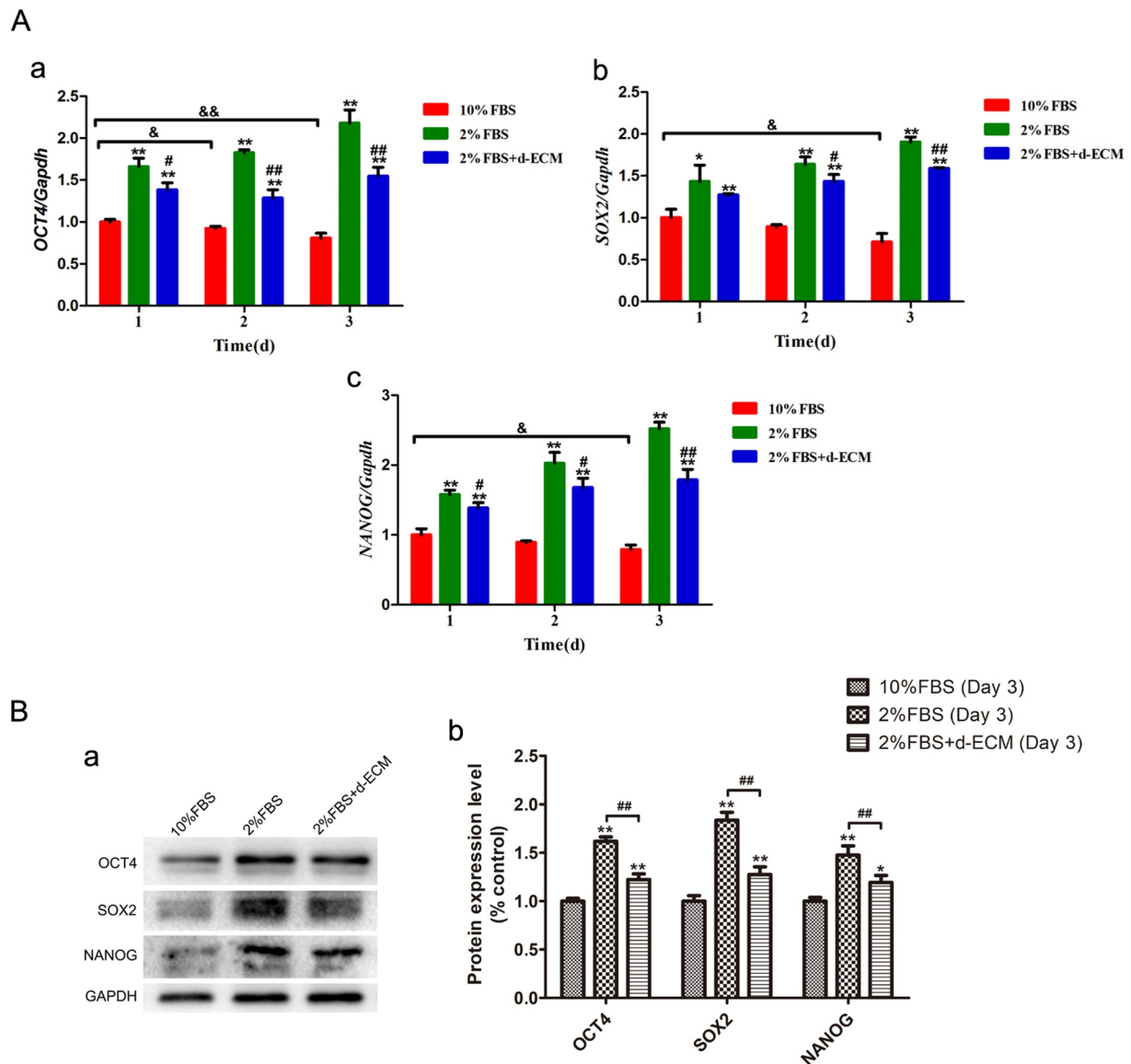


Figure 4. Expression of stemness-associated genes. A. ADSCs at the 5th passage were inoculated into plates with plastic or d-ECM substrates, and were then cultured in 2% FBS for 3 days in total. Cells cultured in 10% FBS served as control group. The transcription of OCT4 (a), SOX2 (b) and NANOG (c) genes was determined by RT-PCR every day. $N = 3$. *, $p < 0.05$, vs. 10% FBS group; **, $p < 0.01$, vs. 10% FBS group; #, $p < 0.05$, vs. 2% FBS group; ##, $p < 0.01$, vs. 2% FBS group; &, $p < 0.05$, vs. 10% FBS group on day 1; &&, $p < 0.01$, vs. 10% FBS group on day 1. B. The expression of OCT4, SOX2 and NANOG proteins was determined by Western blotting on day 3. Equal loading of proteins was confirmed by GAPDH. $N = 3$. *, $p < 0.05$, vs. 10% FBS group; **, $p < 0.01$, vs. 10% FBS group; ##, $p < 0.01$, vs. 2% FBS group. OCT4, octamer-binding transcription factor-4; SOX2, SRY-related high-mobility-group-box protein-2; NANOG, Nanog homeobox protein.

was regulated neither by d-ECM nor by PD98059 (Figure 5(b)).

Following adipogenic differentiation, Western blotting was performed again for further analysis. Compared to control group (10% FBS), the expression levels of ERK1/2 and PPAR γ decreased in 2% FBS group, while the phosphorylation of both proteins increased. Reseeding cells on the substrates coated with d-ECM reversed the effects of serum-restriction. On the basis of 2% FBS and d-ECM,

pretreating cells with PD98059 unexpectedly up-regulated the phosphorylation of ERK1/2, accompanied by the decreased PPAR γ expression. In addition, the expression of adiponectin and aP2 was highly consistent with PPAR γ under aforementioned conditions (Figure 7). Given the above, we discovered an interesting phenomenon that there was an opposing relationship between the ERK1/2 phosphorylation of undifferentiated and fully differentiated ADSCs.

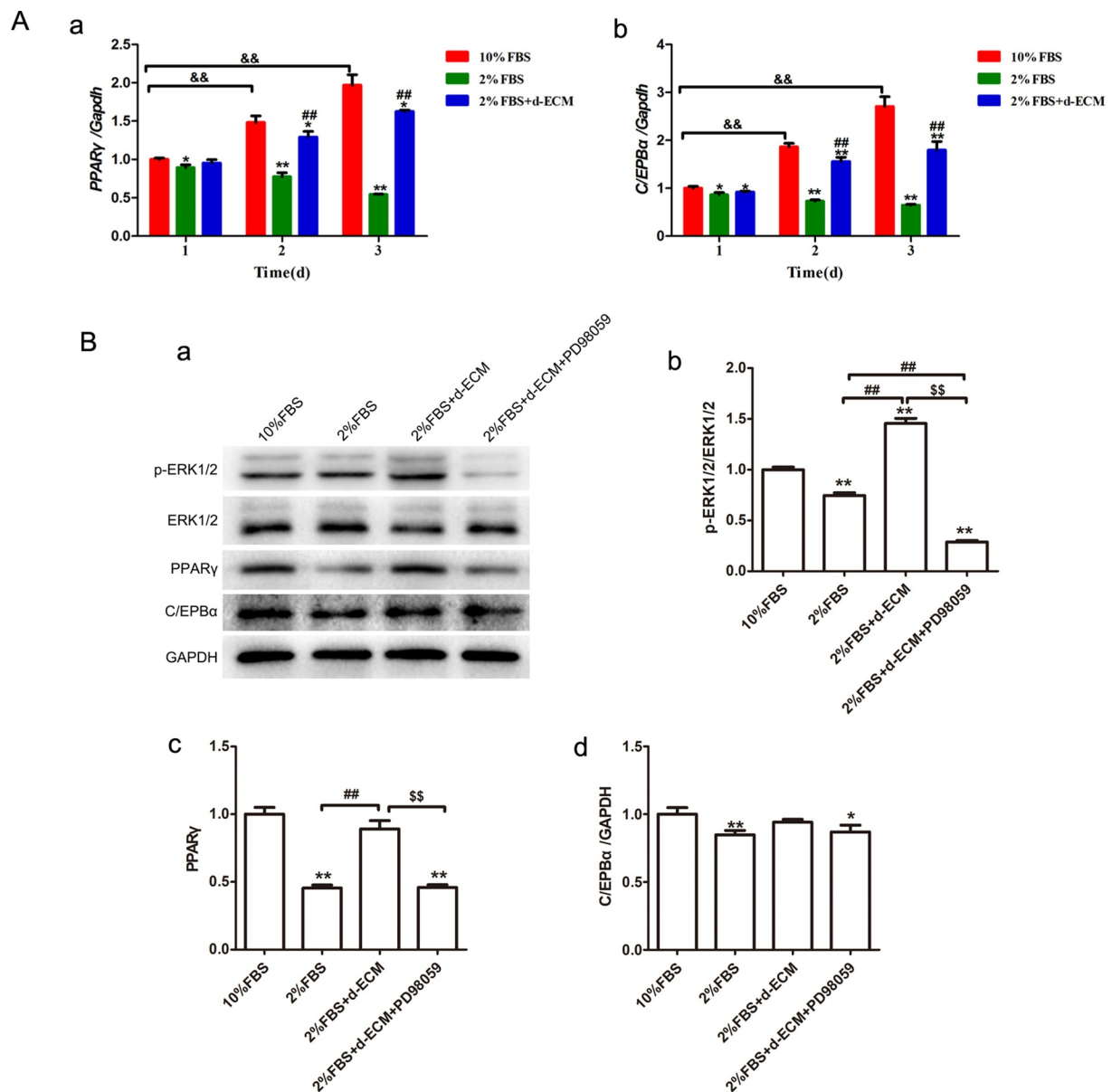


Figure 5. Relation between ERK1/2 and adipogenic genes in the undifferentiated ADSCs. A. ADSCs at the 5th passage were cultured in 2% FBS on the plastic or d-ECM substrates, and the mRNA levels of PPAR γ (a) and C/EPB α (b) were examined on days 1–3, respectively. Cells in 10% FBS were used as control group. N = 3. *, p < 0.05, vs. 10% FBS group; **, p < 0.01, vs. 10% FBS group; ##, p < 0.01, vs. 2% FBS group; &&, p < 0.01, vs. 10% FBS group on day 1. B. ADSCs were treated with 2% FBS and/or d-ECM. Cells without any treatment were set as control. For d-ECM treatment group, a copy pretreated with 50 μ M PD98059 was established to inhibit ERK1/2 signalling (a). Afterwards, the phosphorylation of ERK1/2 (b), and the expression levels of PPAR γ (c) and C/EPB α (d) were examined by Western blotting analysis. Equal loading of proteins was demonstrated by GAPDH. N = 3. *, p < 0.05, vs. 10% FBS group; **, p < 0.01, vs. 10% FBS group; ##, p < 0.01, vs. 2% FBS group; \$\$, p < 0.01, vs. 2% FBS + d-ECM group. P-ERK1/2, phospho-extracellular signal-regulated kinase1/2; ERK1/2, extracellular signal-regulated kinase1/2; PPAR γ , peroxisome proliferators-activated receptor γ ; C/EPB α , CCAAT enhancer-binding proteins.

Differentiation of ADSCs into adipocytes

Compared to control group (10% FBS) and d-ECM group, lipid droplets resembling refractile spheres were almost disappeared in 2% FBS group, and were less but bigger in PD98059 pretreatment group (Figure 6(a)). The result of Oil red O staining showed that there were more fat globules visible when supplemented with

10% FBS or with d-ECM (Figure 6(a)). Relative stained area, mean staining intensity (IntDen/Area) and the absorbance at 540 nm were determined to quantitatively evaluate the adipogenic ability of ADSCs. The decline of these indexes induced by low serum was ameliorated by d-ECM, but aggravated once again by the addition of PD98059 (Figure 6(b)).

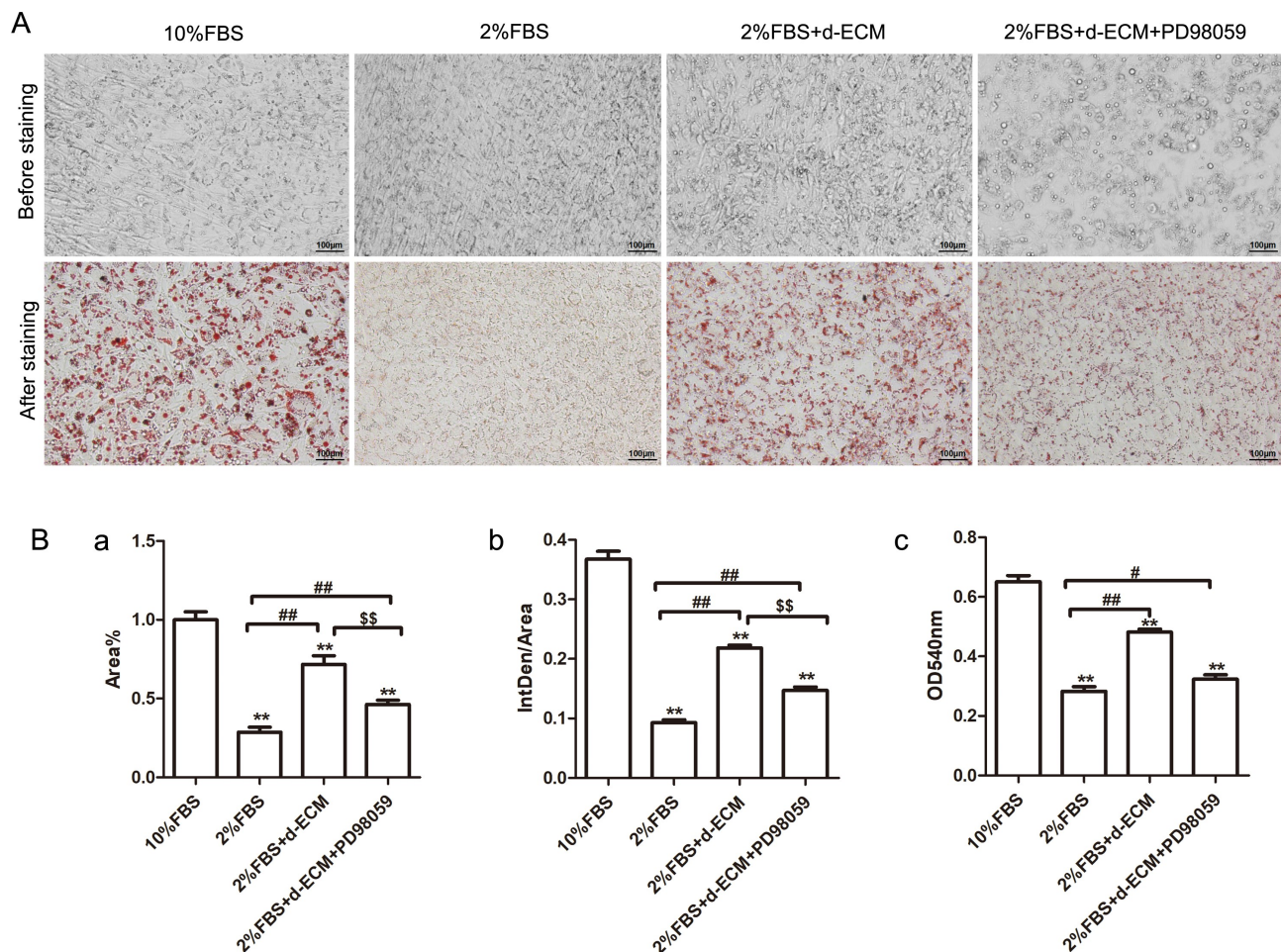


Figure 6. Adipogenic induction and Oil Red O staining. A. As described above, the 5th passage ADSCs with or without PD98059 pretreatment were seeded on the plastic or d-ECM substrates and then cultured in 2% FBS for 3 days, followed by 14-days adipogenic induction and subsequent Oil Red O staining. Cells cultured in complete medium were regarded as the control group. N = 3. Bars = 100 μ m. B. For each group, relative stained area (Area%, a), mean staining intensity (IntDen/Area, b) and optical density at 540 nm (OD540nm, c) after destaining were determined to evaluate the adipogenic ability of ADSCs. **, $p < 0.01$, vs. 10% FBS group; #, $p < 0.05$, vs. 2% FBS group; ##, $p < 0.01$, vs. 2% FBS group; \$\$, $p < 0.01$, vs. 2% FBS + d-ECM group.

Discussion

It was demonstrated in our previous study that the d-ECM substrate could protect ADSCs against H_2O_2 -induced senescence and stimulate cell proliferation [22]. As a natural substance secreted by autologous cells, d-ECM is very safe and has tremendous potential for usage in regeneration medicine [28]. In this study, we reproduced d-ECM by decellularization using the aforementioned method. We found that d-ECM increased viability and proliferation of the reseeded ADSCs in low serum culture (Figure 3(a-c)), which was in agreement with previous results [29]. It has been demonstrated that bioactive components in extracellular matrix can promote cell proliferation and differentiation through ERK1/2 signalling pathway [20,21,30]. In addition, the ERK1/2 pathway is proved to be required for serum-stimulated DNA synthesis [31], and sustained activation of ERK1/2 is related to

the mitogenic potential of growth factors [32]. Therefore, we hypothesize that the ERK1/2 pathway may be involved in the positive effect of d-ECM on serum-restricted ADSCs.

Under the condition without any interference (10% FBS), the transcript levels of stemness-associated genes were decreased over time (Figure 4(a)). In contrast, the adipogenic genes increased during this process (Figure 5(a)). It suggested that there was a tendency of spontaneous adipogenesis in ADSCs cultured in growth medium, which was supported by a previous study where the expression of PPAR γ in MSCs relied on serum rather than any differentiation inducers [3]. Moreover, we found that serum-restriction decreased this tendency while d-ECM increased it. At the beginning of adipocyte differentiation process, preadipocytes will undergo a proliferative period called mitotic clonal expansion (MCE) [33]. Yu et al. found that arresting

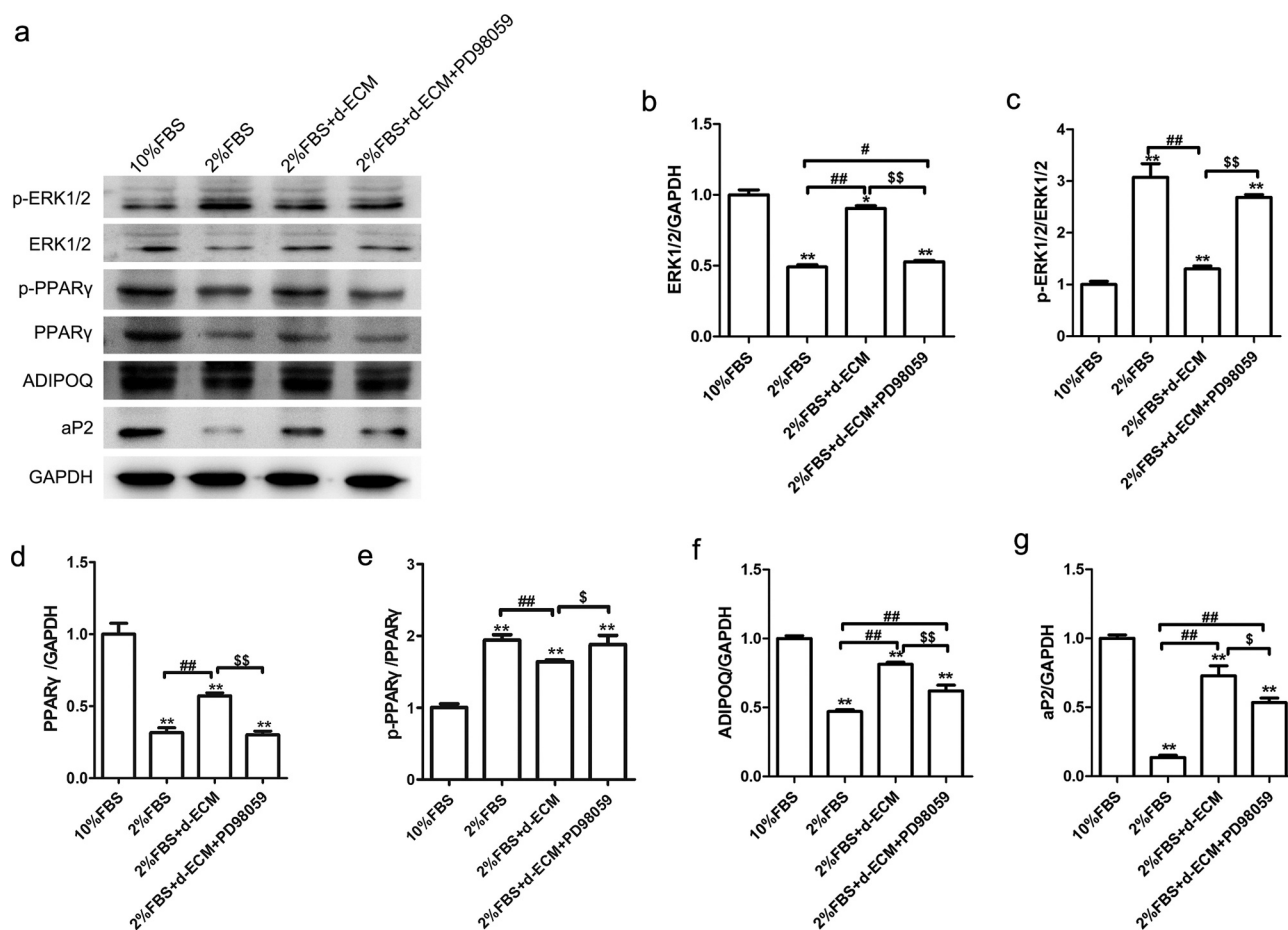


Figure 7. Effects of d-ECM on the ERK1/2-PPAR γ pathway and the expression of adipocyte secreting factors ADIPOQ and aP2 in the fully differentiated ADSCs. After 3-days treatments and 14-days adipogenic induction, ADSCs at the 5th passage were collected and used for Western blotting analysis (a). Protein levels of ERK1/2 (b), p-ERK1/2 (c), PPAR γ (d), p-PPAR γ (e), ADIPOQ (f) and aP2 (g) were examined. GAPDH demonstrated the equal loading of protein samples. N = 3. *, p < 0.05, vs. 10% FBS group; **, p < 0.01, vs. 10% FBS group; #, p < 0.05, vs. 2% FBS group; ##, p < 0.01, vs. 2% FBS group; \$, p < 0.05, vs. 2% FBS + d-ECM group; \$\$, p < 0.01, vs. 2% FBS + d-ECM group. ADIPOQ, adiponectin; aP2, adipocyte fatty-acid binding protein.

cell cycle and blocking MCE by inula britannica could prevent early differentiation of 3T3-L1 preadipocytes [34]. In the present study, we demonstrated that proliferation and cellular polarity of the uninduced ADSCs reseeded on d-ECM were increased (Figure 3(c,d)), which suggested a possible acceleration of MCE. However, from the perspective of McBeath et al. [35], excessive polarity in the late stage of differentiation was regarded as a feature of poor differentiation, which was consistent with what was observed in ADSCs in the 2% FBS group (Figure 6(a)).

In the present study, it was demonstrated that ADSCs reseeded on d-ECM continuously expressed PPAR γ at higher level compared to those on the plastic substrates whether the cells were adipogenically induced or not (Figure 5(b), Figure 7). The expression of aP2 and adiponectin, and the adipogenic differentiation of ADSCs were also facilitated by d-ECM treatment (Figure 6, Figure 7). However, the changes of ERK1/2 phosphorylation were

opposite before and after adipogenic differentiation (Figure 5(b), Figure 7). This inconsistency was reflected in the previous studies where the ERK1/2 pathway regulated cell adipogenesis differently. On the one hand, it was reported that activation of the ERK1/2 positively regulated the expression of PPAR and C/EPB and promoted adipogenic differentiation of preadipocytes or MSCs [36,37]. On the other hand, Font de Mora et al. discovered that the phosphorylation of ERK1/2 was not necessary for adipogenesis and even antagonized it [38].

The modulation effects of ERK1/2 on cell proliferation and differentiation are stage-dependent, and phosphorylation of ERK1/2 at different time points produces different adipogenic efficiency [39]. Engelman et al. discovered that activation of MAPK including ERK1/2 only occurred in the early stage of adipogenesis (PMID: 9,822,687). Up-regulation of ERK1/2 pathway at this time can increase PPAR γ expression and initiate adipogenic differentiation, and vice versa [40,41]. On the contrary,

the dephosphorylation of ERK1/2 happens spontaneously in the later stages. This inactivation can be induced by dual specificity phosphatase 1 (DUSP1) [42]. Sustained phosphorylation of ERK1/2 inhibits protein expression of PPAR γ through phosphorylating it at Serine-82 and 112 sites, thereby hindering adipogenic differentiation [43,44]. Based on the above findings and our data, we speculate that d-ECM may promote PPAR γ expression and accelerate adipogenesis by successively increasing and decreasing ERK1/2 phosphorylation during the induction.

In addition, we noticed that PD98059 inhibited ERK1/2 activation and PPAR γ expression in the uninduced ADSCs (Figure 5(b)), which was consistent with the previous study [3]. However, the phosphorylation of ERK1/2 in the terminally differentiated cells was significantly increased in PD98059 pretreatment group (Figure 7), despite the inhibited adipogenesis. Meanwhile, we found that the corresponding cells had rounder bodies, contained bigger lipid droplet (Figure 6(a)), and expressed less adiponectin and aP2 proteins (Figure 7). These phenomenon suggested the formation of hypertrophied adipocytes, whose ERK1/2 phosphorylation level was higher than the normal ones [45]. Therefore, we speculate that the early inhibition of ERK1/2 by PD98059 might result in abnormal adipogenic differentiation and a delayed compensatory increase in ERK1/2 phosphorylation.

This study has several limitations. Firstly, different from the result of RT-PCR, Western blotting analysis showed that the protein expression of C/EPBa in uninduced ADSCs was not significantly influenced by d-ECM. Also, as one of the downstream targets of ERK1/2 [46], it was not inhibited by PD98059 (Figure 5(b)). It remains to be proved that whether the post-transcriptional regulation and other signalling pathways are involved in the process. Secondly, as an active ingredient mediating cell adhesion to extracellular matrix, laminin (LM) was reported to regulate the osteogenic differentiation of dental follicle cells by targeting integrins α 2 and β 1 [47]. Decellularization in this study significantly reduced the LM content (Figure 2), which possibly impaired the LM-associated effect on the adipogenesis of ADSCs. In addition, it was demonstrated that other collagen species and glycoproteins as well as various growth factors existed in the decellularized adipose tissue (DAT) [48]. Mechanisms underlying the effects of these bioactive molecules need to be confirmed in the future experiments. Last but not least, we found that there were an early alternation between the transcriptions of pluripotent genes and adipogenic genes (days 1–3), and a subsequent inconsistency of ERK1/2 phosphorylation during the adipogenesis of ADSCs (day 3 vs. day 14). However, Pauken et al. discovered that many matrix

components including COL1, COL4, FN and LM could obviously up-regulate ERK1/2 phosphorylation within 90 min, which wore off in the later periods [49]. Therefore, precise determination of ERK1/2 phosphorylation at more and earlier time points may help to further reveal the role of ERK1/2 pathways on the d-ECM-induced adipogenesis promotion of ADSCs.

In conclusion, we demonstrated that autologous d-ECM ameliorated adipogenic differentiation of ADSCs in low serum culture by a stage-dependent regulation on ERK1/2-PPAR γ pathway. We believe this result support an idea that increasing ECM components around cells may bring the superiority of ADSCs into full play in the field of regeneration medicine.

Disclosure statement

The authors declare that they have no conflicts of interest to report regarding the present study.

Funding

This research was funded by National Natural Science Foundation of China [81971850], Wenzhou Municipal Science and Technology Bureau [Y20190017], Wenzhou Municipal Science and Technology Bureau [Y20180148], and Wenzhou Municipal Science and Technology Bureau [Y2020085].

Ethics approval and consent to participate

This study was approved by the Research Ethics Committee of Wenzhou Medical University.

ORCID

Yao Qian  <http://orcid.org/0000-0003-2008-4160>

References

- [1] Mizuno H, Tobita M, Uysal AC. Concise review: adipose-derived stem cells as a novel tool for future regenerative medicine. *Stem Cells*. 2012;30(5):804–810.
- [2] Potier E, Ferreira E, Meunier A, et al. Prolonged hypoxia concomitant with serum deprivation induces massive human mesenchymal stem cell death. *Tissue Eng*. 2007;13(6):1325–1331.
- [3] Wu L, Cai X, Dong H, et al. Serum regulates adipogenesis of mesenchymal stem cells via MEK/ERK-dependent PPAR γ expression and phosphorylation. *J Cell Mol Med*. 2010;14(4):922–932.
- [4] Fani N, Ziadlou R, Shahhoseini M, et al. Comparative epigenetic influence of autologous versus fetal bovine serum on mesenchymal stem cells through in vitro osteogenic and adipogenic differentiation. *Exp Cell Res*. 2016;344(2):176–182.

- [5] Zhang Z, Qu R, Fan T, et al. Stepwise adipogenesis of decellularized cellular extracellular matrix regulates adipose tissue-derived stem cell migration and differentiation. *Stem Cells Int.* 2019;1845926. DOI:10.1155/2019/1845926.
- [6] Lee MK, Lin SP, HuangFu WC, et al. Endothelial-derived extracellular matrix ameliorate the stemness deprivation during ex vivo expansion of mouse bone marrow-derived mesenchymal stem cells. *PLoS One.* 2017;12(8):e0184111.
- [7] Rakian R, Block TJ, Johnson SM, et al. Native extracellular matrix preserves mesenchymal stem cell “stemness” and differentiation potential under serum-free culture conditions. *Stem Cell Res Ther.* 2015;6(1):235.
- [8] Tang C, Jin C, Xu Y, et al. Chondrogenic differentiation could be induced by autologous bone marrow mesenchymal stem cell-derived extracellular matrix scaffolds without exogenous growth factor. *Tissue Eng Part A.* 2016;22(3–4):222–232.
- [9] Guneta V, Loh QL, Choong C. Cell-secreted extracellular matrix formation and differentiation of adipose-derived stem cells in 3D alginate scaffolds with tunable properties. *J Biomed Mater Res.* 2016;104(5):1090–1101.
- [10] Nguyen TT, Scimeca JC, Filloux C, et al. Co-regulation of the mitogen-activated protein kinase, extracellular signal-regulated kinase 1, and the 90-kDa ribosomal S6 kinase in PC12 cells. Distinct effects of the neurotrophic factor, nerve growth factor, and the mitogenic factor, epidermal growth factor. *J Biol Chem.* 1993;268:9803–9810.
- [11] Pogrmic-Majkic K, Samardzija Nenadov D, Fa S, et al. BPA activates EGFR and ERK1/2 through PPAR γ to increase expression of steroidogenic acute regulatory protein in human cumulus granulosa cells. *Chemosphere.* 2019;229:60–67.
- [12] Aubert J, Belmonte N, Dani C. Role of pathways for signal transducers and activators of transcription, and mitogen-activated protein kinase in adipocyte differentiation. *Cell Mol Life Sci.* 1999;56(5–6):538–542.
- [13] Bost F, Aouadi M, Caron L, et al. The role of MAPKs in adipocyte differentiation and obesity. *Biochimie.* 2005;87(1):51–56.
- [14] Teven CM, Liu X, Hu N, et al. Epigenetic regulation of mesenchymal stem cells: a focus on osteogenic and adipogenic differentiation. *Stem Cells Int.* 2011;2011:201371.
- [15] Gao G, Li H, Huang Y, et al. Periodic mechanical stress induces extracellular matrix expression and migration of rat nucleus pulposus cells through Src-GIT1-ERK1/2 signaling pathway. *Cell Physiol Biochem.* 2018;50(4):1510–1521.
- [16] Chen S, Peng C, Wei X, et al. Simulated physiological stretch increases expression of extracellular matrix proteins in human bladder smooth muscle cells via integrin α 4/ β 1-FAK-ERK1/2 signaling pathway. *World j urology.* 2017;35(8):1247–1254.
- [17] Jia P, Hu Y, Li G, et al. Roles of the ERK1/2 and PI3K/PKB signaling pathways in regulating the expression of extracellular matrix genes in rat pulmonary artery smooth muscle cells. *Acta Cir Bras.* 2017;32(5):350–358.
- [18] Li X, Wang L, Ma H. Betaine alleviates high glucose-induced mesangial cell proliferation by inhibiting cell proliferation and extracellular matrix deposition via the AKT/ERK1/2/p38 MAPK pathway. *Mol Med Rep.* 2019;20(2):1754–1760.
- [19] Zhou H, Shen J, Hu Z, et al. Leukemia inhibitory factor promotes extracellular matrix synthesis in degenerative nucleus pulposus cells via MAPK-ERK1/2 signaling pathway. *Biochem Biophys Res Commun.* 2018;507(1–4):253–259.
- [20] Buchert J, Diederichs S, Kreuser U, et al. The role of extracellular matrix expression, ERK1/2 signaling and cell cohesiveness for cartilage yield from iPSCs. *Int J Mol Sci.* 2019;20(17):20.
- [21] Sun T, Yao S, Liu M, et al. Composite scaffolds of mineralized natural extracellular matrix on true bone ceramic induce bone regeneration through Smad1/5/8 and ERK1/2 pathways. *Tissue Eng Part A.* 2018;24(5–6):502–515.
- [22] Yu X, He Y, Chen Z, et al. Autologous decellularized extracellular matrix protects against H₂O₂-induced senescence and aging in adipose-derived stem cells and stimulates proliferation in vitro. *Biosci Rep.* 2019;39. DOI:10.1042/BSR20182137.
- [23] Kwak DH, Lee JH, Kim T, et al. *Aristolochia manshuriensis* Kom inhibits adipocyte differentiation by regulation of ERK1/2 and Akt pathway. *PLoS One.* 2012;7(11):e49530.
- [24] Hatzmann FM, Ejaz A, Wieggers GJ, et al. Quiescence, stemness and adipogenic differentiation capacity in human DLK1/CD34/CD24 adipose stem/progenitor cells. *Cells.* 2021;10(2):10.
- [25] Qian Y, Wang JP, Ji ZW, et al. Acetyl-L-carnitine protects adipose-derived stem cells exposed to H₂O₂ through regulating AMBRA1-related autophagy. *Biocell.* 2021;45(1):189–198.
- [26] Wagner W, Horn P, Castoldi M, et al. Replicative senescence of mesenchymal stem cells: a continuous and organized process. *PLoS One.* 2008;3(5):e2213.
- [27] He Y, Yu X, Chen Z, et al. Stromal vascular fraction cells plus sustained release VEGF/Ang-1-PLGA microspheres improve fat graft survival in mice. *J Cell Physiol.* 2019;234(5):6136–6146.
- [28] Przybyt E, Van Luyn MJ, Harmsen MC. Extracellular matrix components of adipose derived stromal cells promote alignment, organization, and maturation of cardiomyocytes in vitro. *J Biomed Mater Res.* 2015;103(5):1840–1848.
- [29] Kim JH, Shin SH, Li TZ, et al. Influence of in vitro biomimicked stem cell ‘niche’ for regulation of proliferation and differentiation of human bone marrow-derived mesenchymal stem cells to myocardial phenotypes: serum starvation without aid of chemical agents and prevention of spontaneous stem cell transformation enhanced by the matrix environment. *J tissue eng regener med.* 2016;10(1):e1–13.
- [30] Tao Y, Zhou X, Liu D, et al. Proportion of collagen type II in the extracellular matrix promotes the differentiation of human adipose-derived mesenchymal stem

- cells into nucleus pulposus cells. *Biofactors*. 2016;42(2):212–223.
- [31] Sale EM, Atkinson PG, Sale GJ. Requirement of MAP kinase for differentiation of fibroblasts to adipocytes, for insulin activation of p90 S6 kinase and for insulin or serum stimulation of DNA synthesis. *EMBO J*. 1995;14(4):674–684.
- [32] Meloche S, Seuwen K, Pagès G, et al. Biphasic and synergistic activation of p44mapk (ERK1) by growth factors: correlation between late phase activation and mitogenicity. *Mol Endocrinol*. 1992;6(5):845–854.
- [33] Tang QQ, Otto TC, Lane MD, et al. Mitotic clonal expansion: a synchronous process required for adipogenesis. *Proc Natl Acad Sci*. 2003;100(1):44–49.
- [34] Yu HS, Kim WJ, Bae WY, et al. Inula britannica inhibits adipogenesis of 3T3-L1 preadipocytes via modulation of mitotic clonal expansion involving ERK 1/2 and akt signaling pathways. *Nutrients*. 2020;12(10):12.
- [35] McBeath R, Pirone DM, Nelson CM, et al. Cell shape, cytoskeletal tension, and RhoA regulate stem cell lineage commitment. *Dev Cell*. 2004;6(4):483–495.
- [36] Prusty D, Park BH, Davis KE, et al. Activation of MEK/ERK signaling promotes adipogenesis by enhancing peroxisome proliferator-activated receptor gamma (PPARgamma) and C/EBP alpha gene expression during the differentiation of 3T3-L1 preadipocytes. *J Biol Chem*. 2002;277(48):46226–46232.
- [37] Xu B, Ju Y, Song G, et al. Role of p38, ERK1/2, focal adhesion kinase, RhoA/ROCK and cytoskeleton in the adipogenesis of human mesenchymal stem cells. *J Biosci Bioeng*. 2004;117(5):624–631.
- [38] Font de Mora J, Porrás A, Ahn N, et al. Mitogen-activated protein kinase activation is not necessary for, but antagonizes, 3T3-L1 adipocytic differentiation. *Cell Mol Biol*. 1997;17:6068–6075.
- [39] Engelman JA, Lisanti MP, Scherer PE. Specific inhibitors of p38 mitogen-activated protein kinase block 3T3-L1 adipogenesis. *J Biol Chem*. 1998;273(48):32111–32120.
- [40] Bost F, Caron L, Marchetti I, et al. Retinoic acid activation of the ERK pathway is required for embryonic stem cell commitment into the adipocyte lineage. *Biochem J*. 2002;361(3):621–627.
- [41] Gwon SY, Ahn JY, Jung CH, et al. Shikonin suppresses ERK 1/2 phosphorylation during the early stages of adipocyte differentiation in 3T3-L1 cells. *BMC complementary altern med*. 2013;13(1):207. .
- [42] Ferguson BS, Nam H, Stephens JM, et al. Mitogen-dependent regulation of DUSP1 governs ERK and p38 signaling during early 3T3-L1 adipocyte differentiation. *J Cell Physiol*. 2016;231(7):1562–1574.
- [43] Camp HS, Tafuri SR. Regulation of peroxisome proliferator-activated receptor gamma activity by mitogen-activated protein kinase. *J Biol Chem*. 1997;272(16):10811–10816.
- [44] Hu E, Kim JB, Sarraf P, et al. Inhibition of adipogenesis through MAP kinase-mediated phosphorylation of PPARgamma. *Science*. 1996;274(5295):2100–2103.
- [45] Malekpour-Dehkordi Z, Teimourian S, Nourbakhsh M, et al. Metformin reduces fibrosis factors in insulin resistant and hypertrophied adipocyte via integrin/ERK, collagen VI, apoptosis, and necrosis reduction. *Life Sci*. 2019;233:116682.
- [46] Aubert J, Dessolin S, Belmonte N, et al. Leukemia inhibitory factor and its receptor promote adipocyte differentiation via the mitogen-activated protein kinase cascade. *J Biol Chem*. 1999;274(35):24965–24972.
- [47] Viale-Bouroncle S, Gosau M, Morscheck C. Laminin regulates the osteogenic differentiation of dental follicle cells via integrin- α 2/- β 1 and the activation of the FAK/ERK signaling pathway. *Cell Tissue Res*. 2014;357(1):345–354.
- [48] Mohiuddin OA, Campbell B, Poche JN, et al. Decellularized Adipose Tissue: biochemical Composition, in vivo Analysis and Potential Clinical Applications. *Ad exp med biol*. 2020;1212:57–70.
- [49] Pauken CM, Caplan MR. Temporal differences in Erk1/2 activity distinguish among combinations of extracellular matrix components. *Acta Biomater*. 2011;7(11):3973–3980.